Multi-objective optimisation of a magnetic gear for powertrain applications

Terms of use:

Publisher copyright

(Article begins on next page)

23 April 2024

Multi-objective Optimisation of a Magnetic Gear for Powertrain Applications

Vincenzo Cirimele[1]*, Luca Dimauro[2], Maurizio Repetto[1], Elvio Bonisoli[2]

Politecnico di Torino, Corso Duca degli Abruzzi, 24, 10129, Torino, Italy

[1] DENERG, Department of Energy 'Galileo Ferraris"

[2] DIMEAS, Department of Mechanical and Aerospace Engineering

Abstract

This paper proposes the study of a magnetic gear by means of multi-objective optimisation. Magnetic gears are structures able to transfer motion between two or more mechanical axles with a given speed ratio. In this aspect they are analogous to a classical mechanical gear but they allow to transfer motion without contact between the moving parts. To replace a standard mechanical gear in an automotive powertrain, the design of a magnetic gear able to transfer the torque needed by the application is required. At the same time, beside the torque, the replacement of the mechanical gear should not alter the dynamic of the powertrain so that also mechanical parameters, as for instance the moment of inertia, must be considered in the design. To cope with these requirements, a multi-objective optimisation approach is proposed that maximises the transmitted torque per unit mass of the magnetic gear while minimising the moment of inertia of the moving parts. Due to the computational intensive evaluation of the magnetic performance, the optimisation is carried out by a deterministic optimisation algorithm coupled to a weighted sum approach of objectives. Results are discussed and compared with those of a commercial application.

Index terms— Electromechanics, magnetic gears, multi-objective optimization, automotive

1   Introduction

Magnetic gears are passive structures where motion is transferred between different axles by the interactions of magnetic flux waves rotating in the air gaps. The rotating flux waves are usually obtained by two sets of rotating permanent magnets, one inner and one outer, creating a different number of poles. The interaction of these two rotating flux waves is modulated by a third part made of a number of ferromagnetic pieces placed in the middle between the two permanent magnet arrays. The resulting action is a transfer of torque between the two permanent magnet parts and a rotation speed that depends on the combination of the number of the interacting magnetic poles [1].

---

*Corresponding author Vincenzo Cirimele, email: vincenzo.cirimele@polito.it

There are different advantages and drawbacks that must be investigated before the adoption of magnetic gears in mechanical transmission systems: one advantage is the possibility to transfer torque in a contactless way, avoiding wearing of the mechanical parts in contact, largely reducing noise and other negative effects. In addition, the absence of contact removes the need of a clutch device limiting the maximum stress acting on the system. Also efficiencies of the magnetic gears are higher that those of mechanical ones [2]. On the other side, to get the same performances, the volumes of mechanical and magnetic gears are different: mechanical gears are compact due to the high local force values between teeth while magnetic counterparts must rely of higher lever arm values to transfer torque, so they are usually larger than the classical ones.

A design procedure of magnetic gears must necessarily rely on numerical magnetic field analysis: different effects like the shape of the magnetic flux around the ferromagnetic poles, the local saturation of the ferromagnetic materials and, in general, the complex shape of flux distribution are not easily dealt by analytical methods so that usually two-dimensional finite elements tools are employed [3].

Starting from these assumptions, the optimisation of one magnetic gear able to replace a planetary mechanical one in the powertrain of a hybrid car has been setup. The torque transfer requirements of the gear have been defined by the technical report [4] that presents data on one of the most diffuse hybrid cars. The preliminary analyses performed allowed to point out that magnetic gears can be a valid replacement for the planetary gears as concerns torque transmission but highlighted also that volumes in the magnetic counterparts are higher and that mass distribution can create possible problems to the rotational dynamics of the powertrain. As a consequence, the need for the multi-objective optimisation of the system arose, calling for the maximisation of the transmitted torque while minimising at the same time the moment of inertia of the rotating parts.

Optimisation of the structure must rely on the evaluation of the two objectives: torque and moment of inertia as function of the geometrical parameters used to describe the structure. While the moment of inertia can be defined on bare geometry and mass density data of all parts, the evaluation of torque must rely on a nonlinear numerical analysis of the structure. In addition, to keep the study as general as possible, instead of maximising the torque value, its mass density, that is the torque divided by the mass of the structure, is considered. This assumption allows to compare different geometrical structures in an easier way.

Previous studies of the magnetic gear have pointed out that a two dimensional analysis is sufficient to get the evaluation of the main parameters of the magnetic structure [3]. Thus the evaluation of the maximum transmissible torque requires the solution of one finite element two dimensional nonlinear problem.

Due to the computational cost of the analysis the optimisation process has been carried out by a deterministic algorithm exploiting a weighted sum of the objectives and, under the hypothesis of convexity, an exploration of the Pareto front is performed by changing the weights [5].

In the following the main steps of the study are described. In Section 2 a description of the magnetic gear structure is presented together with some data about the powertrain application and its constraints and requirements. Afterwards, the magnetic finite element model that computes the torque is

explained in Section 3 and the proposed optimisation approach is described in Section 4 and Section 5. Finally, the results of the optimisation are discussed and some preliminary conclusions are drawn.

2   Planetary and Magnetic gears

A sketch of a mechanical planetary gear with its main three parts is reported in Fig. 1: the sun gear, the planetary gears, generally three of them that are connected by a carrier, and the ring gear. The structure has 2 degrees of freedom, therefore in order to completely define its kinematics it is necessary to know the rotational speed of at least two elements (for example sun and ring) and then evaluate the other velocity (carrier).

[Figure 1 about here.]

If the carrier part is kept fixed in space, the ratio between the two angular speeds of sun and ring is constrained by the number of teeth of the two cogs Z_r and Z_s ring and sun respectively:

$$\tau_{s/r} = -\frac{Z_r}{Z_s} \tag{1}$$

A similar gear structure can be realised also by a magnetic configuration where the sun and the ring are made by two rotors carrying permanent magnet arrays and ferromagnetic yokes for flux closing. Between the two rotors, a ring of ferromagnetic poles is set whose task is to modulate the two magnetic flux waves rotating in the air gaps. In Fig. 2 a sketch of a magnetic planetary gear is reported.

If the flux modulator is kept stationary, and the one of the two rotors is being driven, the magnetic gear ratio is governed by the following equations [1]:

$$\begin{cases} G_r = -\frac{p - n_s}{n_s} = -\frac{n_r}{n_s} \\ p = n_s + n_r \end{cases} \tag{2}$$

where:

- p is the number of poles of ferromagnetic modulation ring;

- n_s is the number of pole-pairs in the inner rotor (sun);

- n_r is the number of pole-pairs in the outer rotor (ring);

It is apparent that this result is similar to the one obtained in (1).

[Figure 2 about here.]

Planetary gears can be used in the powertrain of a hybrid vehicle where two or more sources of power/energy are combined in order to obtain the required power necessary to propel the car [4]. These vehicles combine the internal combustion engine (ICE) with an electric traction motor that is powered from a secondary storage device, that generally is a battery pack. The planetary gear is used as a power split device allowing to have two torque sources applied to the main mechanical axle.

3 Evaluation of torque in a magnetic gear

As it has been previously pointed out, the performance of a magnetic gear can be evaluated by a two dimensional finite element method taking into account non linearities of the ferromagnetic regions of the gear.

The analysis is performed by means of a magneto-static solution of the structure. The relative motion of the parts should call for a dynamic solution as time-varying magnetic flux can induce eddy currents in conductive parts and losses in ferromagnetic materials. A previous study of the magnetic gear highlighted that these phenomena can be, in a preliminary study, neglected [3]. Nonlinearity in ferromagnetic phenomena is instead correctly taken into account as this effect is of primary importance. Saturation can be in fact critical in ferromagnetic yokes since their magnetic reluctance influences the magnetic flux magnitude created by the permanent magnets and, consequently, the torque.

The torque transmitted between the parts is computed, in the post-processing phase, through the Maxwell's stress tensor. Torque is evaluated along different shell-paths on the two air-gap of the machine and results are then averaged [6]. As a result, each torque evaluation in a particular angular position requires a FEM evaluation.

Since the value of the torque depends on the relative position of the three magnetic parts, its behaviour must be evaluated in a significant number of angular positions. Under the hypothesis that the steel pole pieces are fixed, each configuration is identified by the angle of the sun (θ_s) and that of the ring (θ_r). The discretisation of these two angles should be tiny enough to have a good reconstruction of the torque. In Fig. 3 the map of the torque as function of θ_s and θ_r for $n_s = 5$ and $n_r = 18$ is reported. As it can be guessed by Fig. 3, machine periodicity can be exploited to reduce the number of FEM runs needed to evaluate the torque in any of the relative angular locations. This periodicity derives from the kinematic of the gear, in fact each point at constant torque repeats with periodicity $\tau_s = 360°/n_s = 72°$ (along the y axis in figure) and $\tau_r = 360°/n_r = 20°$ (along the x axis) and the slope of each curve at constant torque is equal to the gear ratio G_r. As an example, the value of the torque at the points P_1 is the same of that of the points P^* and P' suitably shifted. Hence, it is possible to reconstruct the overall torque-angles map by analysing the magnetic gear starting from a single configuration of one of the two rotors and rotating the other one within one period. An example of this evaluation is provided in Fig. 3(b). It is worth mentioning that, if the topology of the magnetic gear (i.e. n_s, n_r and p) does not change, to get the maximum torque it is possible to run only one FEM simulation with the relative position that gives rise to the maximum torque.

[Figure 3 about here.]

Once the geometric structure of the gear is defined, its moment of inertia can be computed by considering the areas occupied by different materials and assigning to each of them the related mass density. The equivalent moment of inertia of the whole machine is computed by considering the different angular velocities of the parts that are related by the gear ratio G_r:

$$J_{eq} = J_s + \frac{J_s}{G_r} \tag{3}$$

4 Geometrical description of the magnetic gear

The geometrical structure of the magnetic gear is described by the parameters reported in Table 1. In the present study, the number of pole pairs n_r, n_r and steel poles p is kept fixed as this set guarantees a torque ripple low with respect to the maximum torque [7]. During the optimisation, the external radius and axial length of the machine are kept constant and equal to the ones of the reference gear that is used as starting point for the optimisation.

[Table 1 about here.]

5 Multi-objective optimisation

The torque of the gear must be maximised while minimising, at the same time, its moment of inertia. These two objectives are contrasting each other: higher torque values require a larger amount of permanent magnets and this is leading to a large value of the equivalent moment of inertia. Using the Pareto approach, this multi-objective process requires several optimisation runs in order to find out the Pareto front [5]. Instead of using the maximum torque value T as objective, the ratio between the maximum torque and the mass of the structure T_ρ is used. This choice puts a larger effort in optimising the exploitation of the magnetic materials inside the structure.

In order to have an idea on the objective functions landscapes, a preliminary parametric investigation of the objectives changing some geometric parameters have been carried out. The results are summarised in Fig. 7: the behaviour of the objectives appears to be quite regular and well behaved; thus, in order to keep the number of function evaluations low, a zero-order search algorithm Pattern Search [8], that does not make use of any gradient of the objective function with respect to degrees of freedom, has been employed. In addition, even if there is no theoretical proof of convexity of the objective functions, the pattern of the torque versus some of the degrees of freedom is well behaved, thus a first attempt to solve the multi-objective problem is carried out by weighting the objectives.

The optimisation procedure has been run a number of ways by changing the starting point of the search and, in all cases tested, the procedure converged at the same minimum point. This is considered as another validation of the well behaviour of the objective function landscape.

The simulation phases have required an average computational time of 29.6 seconds on a workstation equipped with an Intel Core i7-3770 at 3.4 GHz and 32 GB of RAM.

[Figure 4 about here.]

The multi-objective optimisation problem is scalarised by means of a weighted sum using the parameter α that can vary between 0 and 1:

$$f\left(T_\rho, J_{eq}\right) = max\left[\alpha\frac{T_\rho}{T_{\rho\ ref}} - (1-\alpha)\frac{J_{eq}}{J_{eq\ ref}}\right] \tag{4}$$

Two parameters $T_{\rho\ ref}$ and $J_{eq\ ref}$ are used to normalise the two components of the objective function. These two values are computed from the reference machine (see Table 2) used as starting point of the optimisation.

5

6   Results and discussion

By running several single-objective optimisations changing the value of the α parameter, a Pareto front can be obtained and the contrasting nature of the two objectives can be highlighted.

In Fig. 5 the Pareto front for different values of the weight α is shown together with maximum torque and mass of each point. For clarity sake, the same results are reported in Fig. 6 where the same points belonging to the Pareto front are reported as mass and moment of inertia vs. torque.

In Table 2 three different results of the optimisation, corresponding to $\alpha = 0.1, 0.5, 0.9$, are reported together with the corresponding geometries.

For $\alpha = 0.1$, when the moment of inertia has the larger influence on the scalarised objective function, the optimised configuration has a reduced thicknesses and this penalises the torque. The resulting torque is, in fact, practically one half of the value resulting from other cases and this is mainly due to the occurrence of saturation in the yokes. On the opposite side ($\alpha = 0.9$), the thicknesses of the gear are larger. It is interesting to note that the optimised geometry for $\alpha = 0.9$ and $\alpha = 0.5$ results in different thickness of the inner and outer rotor permanent magnets.

The trajectory of the geometric parameters during the optimisation run is presented in Fig. 7 for the weighting parameter $\alpha = 0.5$.

[Figure 5 about here.]

[Figure 6 about here.]

[Table 2 about here.]

[Figure 7 about here.]

As it can be appreciated by the analysis of Fig. 6, torque density and moment of inertia are conflicting objectives and their weighting leads to strongly different results and configurations where low moment of inertia configurations must face a torque value penalisation due to a reduction of magnet thickness and saturation of the ferromagnetic parts, especially of the yokes. In addition, due to different reluctances of the magnetic path in the inner and outer permanent magnet arrays, a magnetic gear with high torque density value presents different thickness for inner and outer permanent magnets.

By making reference to the technical report [4] where a reference value of maximum torque of 230 N/kg is stated, it is possible to see that the magnetic gear structure is able to transfer this value of torque at the inner rotor. By the analysis of the Pareto front picture, Fig. 5, it is possible to state that the configurations obtained by α values larger than 0.5 satisfy the minimum requirements. It is also apparent that the masses of these configurations are larger than 30 kg which is almost one order of magnitude larger than the corresponding planetary gear.

7   Conclusions

The work performed has been devoted to the analysis of a magnetic gear with the aim of evaluating the replacement of a classical planetary gear. Even if this

study gives only theoretical simulated results, some general conclusions can be drawn.

Firstly, the magnetic gear can be a valid replacement for a power split device as it can transmit the torque requested by the vehicle, on the other hand this can be done only if a complete redesign of the power transmission is performed. Dimensions and masses of the magnetic gear are in fact, larger than the classical one and must be accommodated in a way different from the present layout.

However, it must also be remarked that, despite the larger value of mass, a magnetic gear is able to create also a torque limitation. In fact, if the torque acting on the structure exceeds the maximum value, the two rotors are able to slip without any damage. In the corresponding mechanical structure this protection must be implemented by a clutch device. As a result, further studies on the replacement of both planetary gear and clutch will have to be performed and new comparisons assessed.

The study has been performed by approaching the multi-objective optimisation problem by a weighting average of objectives. Even if the computational cost of evaluation of the magnetic gear performance is not negligible, in the future the use of thorough multi-objective procedure will be implemented in order to assess the quality of the Pareto front obtained.

References

[1] Montague R., Bingham C., Atallah K., Servo control of magnetic gears, *IEEE/ASME Transaction on Mechatronics*, 17(2), 2012, pp. 269-278.

[2] Gerald Jungmayr, Jens Loeffler, Bjoern Winter, Frank Jeske, Wolfgang Amrhein, Magnetic Gear: Radial Force, Cogging Torque, Skewing, and Optimization, *IEEE Transactions on Industry Applications* vol. 52, no. 5, 2016, pp. 3822-3830.

[3] Filippini M., Alotto P., An optimization tool for coaxial magnetic gears, *COMPEL - The international journal for computation and mathematics in electrical and electronic engineering*, vol. 36, no. 5, 2017, pp. 1526-1539.

[4] Olszewski M., ”Evaluation of 2004 Toyota Prius hybrid electric drive system”, Oak Ridge National Laboratory, 2006.

[5] Di Barba P., ”Multiobjective Shape Design in Electricity and Magnetism”, Springer 2010.

[6] Henrotte F., Deliege G., and Hameyer K., The eggshell method for the computation of electromagnetic forces on rigid bodies in 2D and 3D, *CEFC 2002*, Perugia, Italy, April 16-18, 2002.

[7] Atallah K., Calverley S.D., Howe D., "Design, analysis and realisation of a high-performance magnetic gear", *IEE Proceedings - Electric Power Applications*, vol. 151, no. 2, 2004, pp. 135-143.

[8] Hooke R., Jeeves T.A. ”Direct search solution of numerical and statistical problems”. Journal of the ACM, (1961), 8 (2): 212-229.

List of Figures
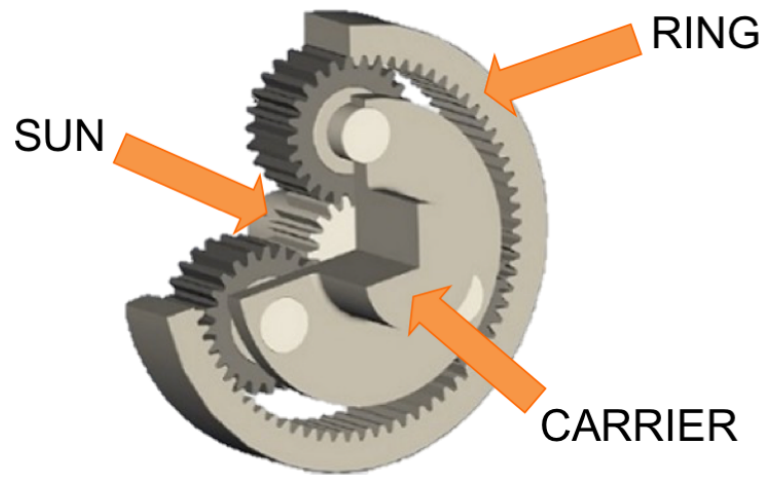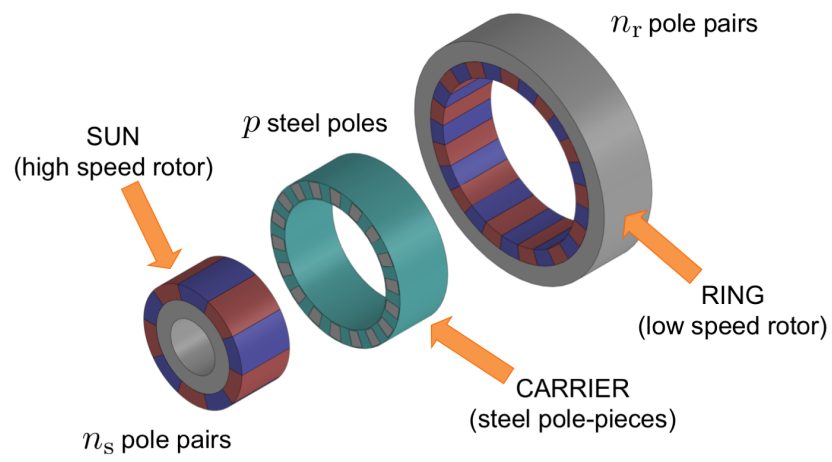
Figure 1: Example of a mechanical planetary gear train.

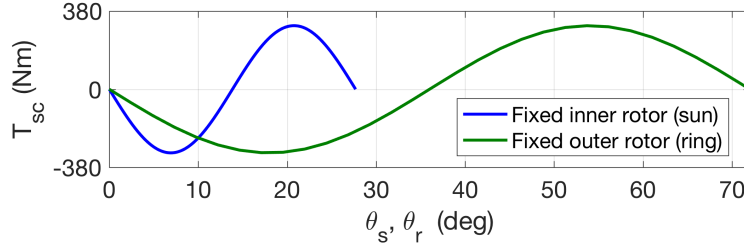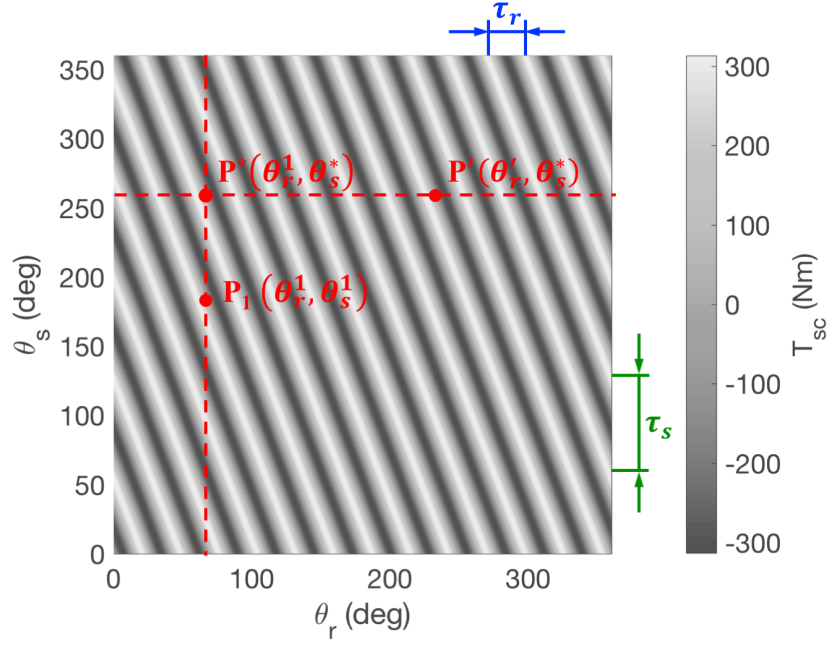Figure 2: Example of a magnetic planetary gear

(a)

(b)

Figure 3: Greyscale map of the sun-carrier torque derived by the simulation of 360×360 relative positions of inner and outer rotor (a). Same torque referred to one period τ_r or τ_s while maintaining fixed the position of one of the two rotors (b).
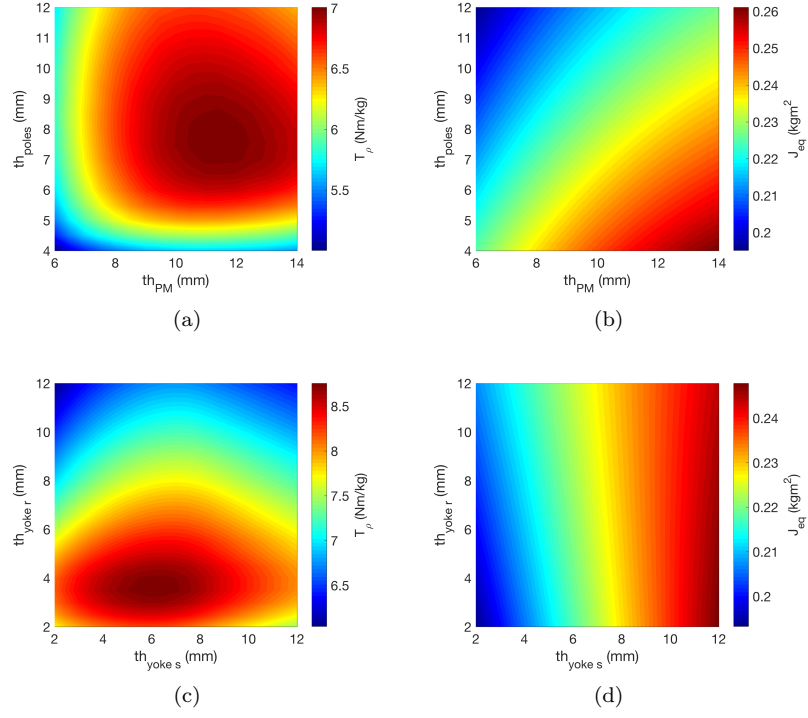
Figure 4: Colormaps of the optimisation goals domains for 2 variables parametric analysis. Torque density versus steel poles and PMs thickness (a). Equivalent moment of inertia versus steel poles and PMs thickness (b). Torque density versus sun and ring rotor thickness (c). Equivalent moment of inertia versus sun and ring rotor thickness (d).
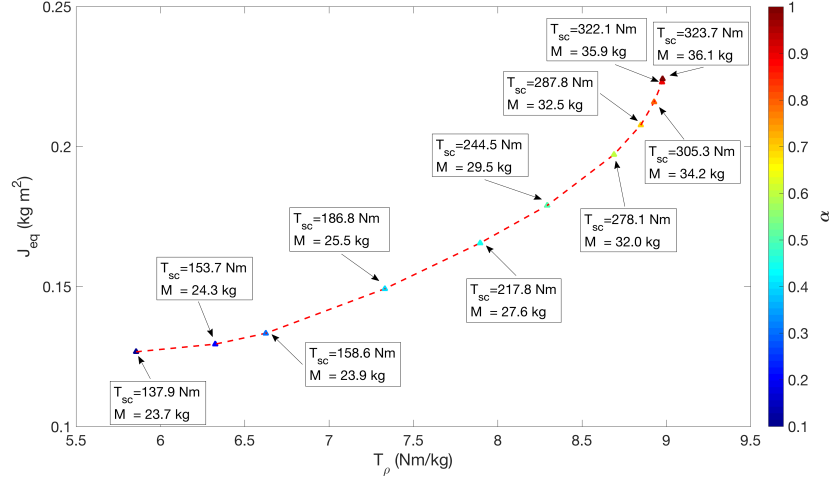
Figure 5: Pareto front for different values of the weight α, the colour of the triangle corresponds to the α value whose scale is reported on the right. For each point of the Pareto front also the corresponding values of mass M and torque T_{sc} are indicated.
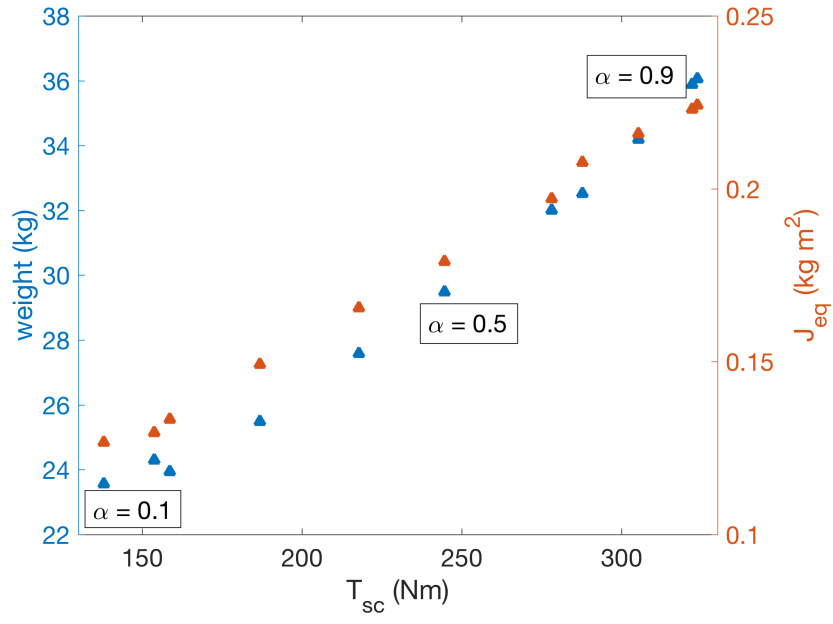
Figure 6: Mass and equivalent moment of inertia of the points belonging to the Pareto front reported as function of the maximum torque.
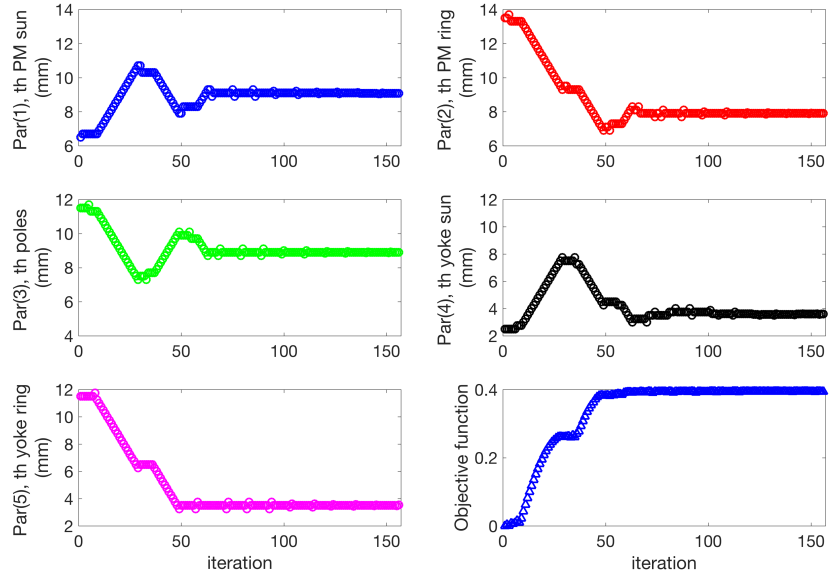
Figure 7: Optimisation variables and objective function evolution for $\alpha = 0.5$.

List of Tables

Table 1: Appearance and parameters of the reference magnetic gear. Fixed parameters in bold.

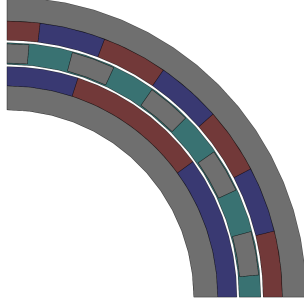| Parameter	Name	Value
Sun yoke thickness	$th_{yoke\ s}$	10 mm
Ring yoke thickness	$th_{yoke\ r}$	10 mm
Sun PM thickness	$th_{PM\ s}$	8 mm
Ring PM thickness	$th_{PM\ r}$	8 mm
Steel poles thickness	th_{poles}	8 mm
Gear external radius	$\boldsymbol{R_{\text{ext}}}$	**125 mm**
Gear axial length	$\boldsymbol{L}$	**200 mm**
Sun PMs pole pairs	$\boldsymbol{n_s}$	**5**
Ring PMs pole pairs	$\boldsymbol{n_r}$	**18**
Carrier steel poles	$\boldsymbol{p}$	**13**

17
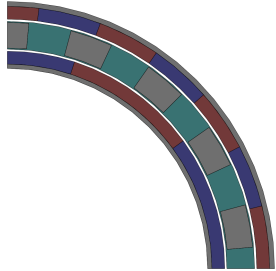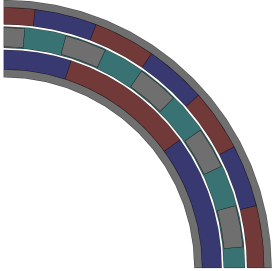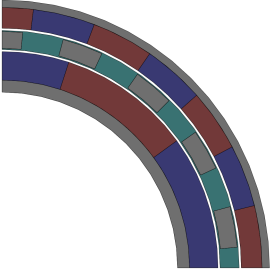
Table 2: Resulting optimised gears for three different values of the weight α.

$\alpha = 0.1$	$\alpha = 0.5$	$\alpha = 0.9$

$\alpha = 0.1$	$\alpha = 0.5$	$\alpha = 0.9$
$th_{PM\ s} = 6$ mm	$th_{PM\ s} = 9.1$ mm	$th_{PM\ s} = 13.3$ mm
$th_{PM\ r} = 6$ mm	$th_{PM\ r} = 7.9$ mm	$th_{PM\ r} = 9.7$ mm
$th_{poles} = 12$ mm	$th_{poles} = 8.9$ mm	$th_{poles} = 7.9$ mm
$th_{yoke\ s} = 2$ mm	$th_{yoke\ s} = 3.6$ mm	$th_{yoke\ s} = 5.6$ mm
$th_{yoke\ r} = 2.3$ mm	$th_{yoke\ r} = 3.5$ mm	$th_{yoke\ r} = 3.5$ mm
$T_\rho = 5.9$ Nm/kg	$T_\rho = 8.3$ Nm/kg	$T_\rho = 9.0$ Nm/kg
$J_{eq} = 0.13$ kg m^2	$J_{eq} = 0.18$ kg m^2	$J_{eq} = 0.22$ kg m^2
$T_{sc} = 137.9$ Nm	$T_{sc} = 244.5$ Nm	$T_{sc} = 322.1$ Nm